Layered structure in compatible binary polymer brushes with high graft density: A computer simulation study

ARTICLE *in* THE JOURNAL OF CHEMICAL PHYSICS · JANUARY 2010

Impact Factor: 2.95 · DOI: 10.1063/1.3299730 · Source: PubMed

4 AUTHORS, INCLUDING:

Hong Liu
Central South University
189 PUBLICATIONS **955** CITATIONS
SEE PROFILE

Xue-Zhang Liang
Jilin University
37 PUBLICATIONS **130** CITATIONS
SEE PROFILE

Layered structure in compatible binary polymer brushes with high graft density: A computer simulation study

Yao-Hong Xue,[1] Hong Liu,[2] Zhong-Yuan Lu,[2,a)] and Xue-Zhang Liang[1]
[1]*Institute of Mathematics, Jilin University, Changchun 130012, China*
[2]*State Key Laboratory of Theoretical and Computational Chemistry, Institute of Theoretical Chemistry, Jilin University, Changchun 130023, China*

(Received 20 October 2009; accepted 7 January 2010; published online 26 January 2010)

We focus on highly grafted binary polymer brushes with compatible components in the cases of different chain lengths. Layered structures parallel to the surface that indicating "phase separation" are observed in a series of dissipative particle dynamics simulations. The stretch parameters indicate that the short chains are suppressed in the lower layer of the film, whereas the longer chains are much stretched in the region dominated by the short chains (lower layer) but possess relaxed conformations in the upper layer. By slightly changing the solvent selectivity to prefer the short chains, we find a reversion of the layered structure. Such a sensitive switch of film property implies its potential application as tuning the wettability and adhesion of the surface in industry. © *2010 American Institute of Physics*. [doi:10.1063/1.3299730]

I. INTRODUCTION

Polymer brushes generally denote layers of polymer chains end-tethered to a solid surface. They give rise to a wide range of important technological and industrial applications.[1–5] In the past decades, a large number of researches[4–35] had been carried out focusing on polymer brushes with different graft densities. With the immobility and nondetachability of the end graft points of the polymer brushes, the systems with binary components often deliver lateral complicated morphology in melt and in solvents[36] which are further used in various applications, such as responsive colloids,[37] coating,[38] protein adsorption,[39] reversibly tunable adhesion, and wettability of surfaces.[40–42] Surfaces covered by the mixed brushes can also be applied for reversible patterning of nanofluidic devices.[43]

Different theoretical studies,[41,44–50] simulations,[51–55] and experiments[56–62] had focused on the immiscible binary polymer brushes, most of which had taken into account the factors such as the solvent quality, graft density, chain length, and incompatibility between species. Marko and Witten[44] first used the self-consistent field theory (SCFT) to predict that a second-order phase transition would occur with the increase of incompatibility between two species in melt binary brushes. They indicated that the two components may segregate laterally into stripes and form the ripple phase. Later, Zhulina and Balazs[50] found a periodical laterally segregated phase at high incompatibility and a homogeneous phase at low incompatibility. In simulation works, Soga *et al.*[53] found more complex lateral structures for polymer brushes in bad solvent. Recently, Wu and the co-workers[54,55] used the Langevin dynamics to study the switch of the phase separation in the binary polymer brush system with the change of solvent quality and the temperature.

In general, the possible morphologies of immiscible binary brushes are the layered state, the ripple state, and the dimple state. The former two types were first proposed by Marko and Witten.[44] The layered structure is constructed with one component enriched near the surface while the other on the top. The ripple structure occurs when the two components self-assemble laterally.[41] The dimple phase was recently pointed out by Minko[41] in which the selective solvent makes the unfavored component form the clusters. Müller[46] and Santer[61] also found the dimple structures in their respective studies.

In most of the studies, these different types of structures are originated from the incompatibility between different species in polymer brushes and the effects of chain configuration entropy are sometimes neglected. Moreover, it is not easy to deal with highly stretched polymer brush in SCFT. So the researches focusing on the effects of chain configuration entropy on polymer brush with high graft density are scarce. To emphasize the importance of chain configuration entropy on the morphology of highly grafted polymer brushes, in this study, we focus on the *compatible* binary polymer brushes immersed in athermal solvent, i.e., there is no energy penalty between different species. In our dissipative particle dynamics (DPD) simulations, we find an interesting kind of entropy driving "phase separation" between the two brush components which is scarcely covered before. Skvortsov *et al.*[63] indicated that the minority shorter brushes in the majority of monodisperse brushes may form slightly deformed coils. In Ref. 64, Merlitz *et al.* pointed out that in the monodisperse system "the removal of just a single monomer leads to a collapse of the chain into the brush and its bond tension disappears entirely." They also showed that "any chemical modification which would shorten the chain length would cause this chain to collapse into the brush and to escape from any further interaction with the brush environment." As a further investigation, in Ref. 65, Merlitz *et al.*

a)Author to whom correspondence should be addressed. Electronic mail: luzhy@jlu.edu.cn.

found that the reversibly switchable surface could be designed by modifying the ends of some minority brush chains among the high density homogeneous system into oversized groups and thermal to the solvent, in which the modified chains would be overstretched above or dive into the brush body with the change of the solvent quality. In this study, we have obtained some comparable interesting results. In the binary brush system with the two components of different chain lengths, we find a trend of phase separation by the emergence of layered structures parallel to the surface. Slight chain length difference between the two components will result in apparent layered structure in the compatible binary polymer brushes. Various stretching features among different types of chains and even in different parts of the same chain imply the diversity of the individual chain conformations. Moreover, the layered structure formed by quasiequal chain lengths is very sensitive on the small change of solvent selectivity which implies the potential application as tuning the wettability and adhesion of the surface in industry. The paper is organized as follows: Sec. II exhibits the simulation details, Sec. III shows the results and the corresponding discussion, and finally, Sec. IV presents the concluding remarks.

II. SIMULATION METHOD AND MODEL CONSTRUCTION

In DPD method, the time evolution of the interacting particles is governed by Newton's equations of motion.[66] Interparticle interactions are characterized by pairwise conservative, dissipative, and random forces acting on a particle i by a particle j. They are given by

$$\begin{aligned}\mathbf{F}_{ij}^{C} &= -\alpha_{ij}\omega^{C}(r_{ij})\mathbf{e}_{ij},\\ \mathbf{F}_{ij}^{D} &= -\gamma\omega^{D}(r_{ij})(\mathbf{v}_{ij}\cdot\mathbf{e}_{ij})\mathbf{e}_{ij},\\ \mathbf{F}_{ij}^{R} &= \sigma\omega^{R}(r_{ij})\xi_{ij}\Delta t^{-1/2}\mathbf{e}_{ij},\end{aligned} \tag{1}$$

where $\mathbf{r}_{ij}=\mathbf{r}_i-\mathbf{r}_j$, $r_{ij}=|\mathbf{r}_{ij}|$, $\mathbf{e}_{ij}=\mathbf{r}_{ij}/r_{ij}$, and $\mathbf{v}_{ij}=\mathbf{v}_i-\mathbf{v}_j$. ξ_{ij} is a random number with 0 mean and unit variance. α_{ij} is the repulsion strength which takes the value of 25 for the particles of same kind in our simulations.[66] The parameter α_{ij} between differing species is often set as larger than 25, representing the degree of compatibility between them. $\omega^{C}(r_{ij})=1-r_{ij}$ for $r_{ij}<1$ and $\omega^{C}(r_{ij})=0$ for $r_{ij}\geq 1$ such that the conservative forces are soft and repulsive. The weight functions $\omega^{D}(r_{ij})$ and $\omega^{R}(r_{ij})$ of the dissipative and random forces couple together to form a thermostat. Español and Warren[67] showed the correct relations between the two functions

$$\begin{aligned}\omega^{D}(r) &= [\omega^{R}(r)]^2,\\ \sigma^2 &= 2\gamma k_B T.\end{aligned} \tag{2}$$

We take a simple choice of $\omega^{D}(r)$ due to Groot and Warren[66]

$$\omega^{D}(r)=[\omega^{R}(r)]^2=\begin{cases}(1-r)^2 & (r<1),\\ 0 & (r\geq 1).\end{cases} \tag{3}$$

It should be noted that the choice of $\omega(r_{ij})$ is not unique and is the simplest form adopted here because of its common usage in roughly all published works.

GW-VV algorithm[66,68] is used for numerical integration,

$$\begin{aligned}\mathbf{r}_i(t+\Delta t) &= \mathbf{r}_i(t)+\Delta t\mathbf{v}_i(t)+1/2(\Delta t)^2\mathbf{f}_i(t),\\ \tilde{\mathbf{v}}_i(t+\Delta t) &= \mathbf{v}_i(t)+\lambda\Delta t\mathbf{f}_i(t),\\ \mathbf{f}_i(t+\Delta t) &= \mathbf{f}_i(\mathbf{r}(t+\Delta t),\tilde{\mathbf{v}}(t+\Delta t)),\\ \mathbf{v}_i(t+\Delta t) &= \mathbf{v}_i(t)+1/2\Delta t(\mathbf{f}_i(t)+\mathbf{f}_i(t+\Delta t)).\end{aligned} \tag{4}$$

We choose $\lambda=0.65$ and $\Delta t=0.05$ here according to Ref. 68.

In our simulations, the radius of interaction, the particle mass, and the temperature are set to be units, i.e., $r_c=m=kT=1$. The particle density ρ is kept equal to 3. Polymers are constructed by connecting the neighboring beads together via the harmonic springs $\mathbf{F}_i^{S}=\Sigma_j C\mathbf{r}_{ij}$. We choose the spring constant $C=10$ according to Ref. 68.

The model used to describe the polymer brush system is composed of two planar walls, the solvent particles and the brush chains end-tethered to the bottom wall. The periodic boundary conditions are applied in both x and y directions. In the z direction, two layers of regularly arranged and densely packed frozen particles are utilized to construct each of the walls. The wall is neutral, namely, there is no incompatibility between the free particles (including the chain monomers and the solvent particles) and the wall particles. This is fulfilled by setting $\alpha_{\mathrm{WW}}=\alpha_{\mathrm{WP}}=25$, in which α_{WW} denotes the interaction parameter between the wall particles and α_{WP} between a free particle and a wall particle. The distance between the two layers in a wall d_L is determined by the density of the wall particles ρ_W, i.e., $d_L=\rho_W^{-1/3}$. ρ_W is a preset parameter, denoting the number of wall particles in unity volume. So d_L is the distance of the neighboring wall particles in x, y, and z directions. Different values of ρ_W correspond to different degrees of the wall roughness whose influence on the polymer brush system had been discussed in detail in our previous work.[69] In the present study, we choose $\rho_W=8$, thus $d_L=0.5$, corresponding to a highly dense and smooth wall. Because the interaction cutoff radius $r_c=1$, the free particles are not able to feel the existence of the wall particles from the third layer. Therefore, the wall can be reasonably described by two closely packed layers of frozen wall particles as shown above. Furthermore, to keep the wall impenetrable, when a free particle hits the wall, a bounce-back reflection condition is imposed so that the particle can move back into the fluid.[70] In the simulations, the uniform distance between the neighboring graft points is set as 1.0 in both x and y directions; this results in a high graft density $\sigma=1$ for the polymer brush (here the graft density is defined as the number of the end-tethered chains, i.e., the number of graft points in the unity area of the grafting surface).

The simulation box size is $L_x=L_y=45$ and L_z (defined as the distance between the top and the bottom wall) is set as a variable depending on the chain lengths so that the brush chains are not able to touch the top wall during the simulations. In practice, we choose $L_z\in\{32,48,64,96,128\}$, consequently the system consists of {194 400, 291 600, 388 800, 583 200, 777 600} movable particles. The types of the graft points (half of which are A and others are B) on the surface are defined randomly, then the chains grow from these graft

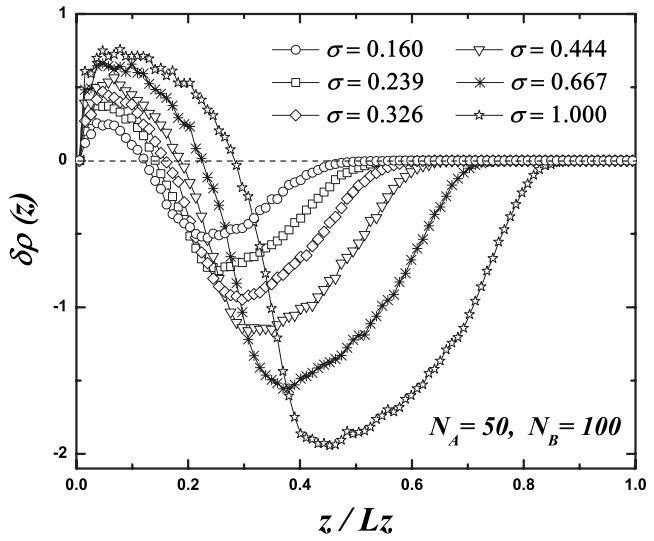

FIG. 1. The variation in the density difference profile of the two species along the z direction $\delta\rho(z)$ as a function of z/Lz in the systems with $N_A=50$ and $N_B=100$ for different graft densities. Five independent samples after equilibrium are chosen to calculate the mean value and the error bar. The error bars are not shown here for clarity.

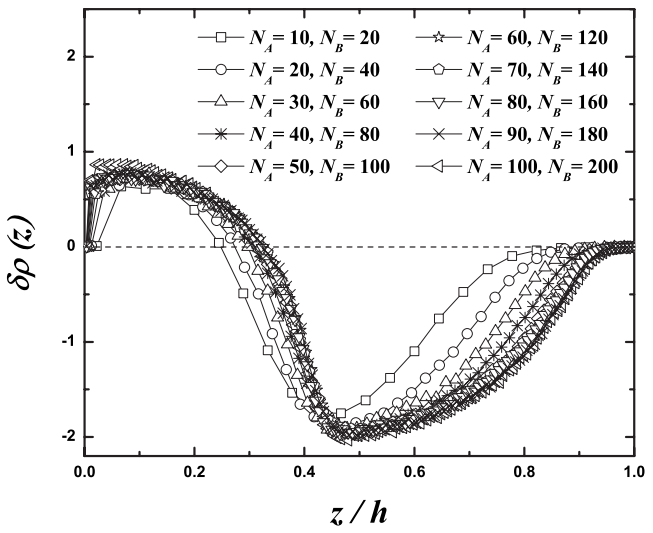

FIG. 2. The variation in the density difference profile of the two species along the z direction $\delta\rho(z)$ as a function of z/h in the systems with $N_A:N_B=1:2$. Five independent samples after equilibrium are chosen to calculate the mean value and the error bar. The error bars are not shown here for clarity.

points to form a binary brush system. After the brush chains are generated, we set all the other free particles in this system as the solvent particles.

The simulations are conducted in canonical ensemble. After generating the initial configuration 2.5×10^5 steps integrations are carried out to ensure that the systems are well relaxed. The equilibrium data are all obtained in the simulations after 2.5×10^5 steps.

III. SIMULATION RESULTS AND DISCUSSION

In the athermal system, all of the interaction parameters are set as 25, i.e., $\alpha_{ij}=25$ where i and j denote arbitrary particles in the system. In the simulations, the only variable factor is the chain length N_A or N_B of each kind of polymer chain.

First, we concentrate on the polymer brushes with $N_A=50$ and $N_B=100$ but with different graft densities. Figure 1 shows the density difference profile of the two species along z direction ($\delta\rho(z)=\rho_A(z)-\rho_B(z)$) under different graft densities. $\rho_A(z)$ and $\rho_B(z)$ are the densities of A and B components along z direction, respectively. Figure 1 apparently shows that the systems possess layered structures, indicating a "phase separation" behavior. The maximum absolute values of $\delta\rho(z)$ can be taken as the degree of phase separation. Therefore it is clear that with increasing graft density, the phase separation becomes more obvious. It is also shown in Fig. 1 that the films with low graft densities are thinner since the brush chain concentrations are lower in these cases. Therefore in these highly constraint systems higher graft density leads to enhanced phase separationlike behavior. In the following, for better understanding the dependence of phase separation on other factors, the high graft density $\sigma=1$ will always be chosen as otherwise indicated. It should be noted that the DPD potential is a kind of soft potential to describe the coarse-grained polymer systems. In DPD, one bead may represent a group of molecules lumped together. Thus different beads can largely overlap with each other. As a result, although the graft density $\sigma=1$ looks fairly high, the system is not really closely packed. We have also validated the bond length distribution in such systems. We find the bond length distributions are very similar with that in the free chain melt, implying that the chains are neither overstretched, nor obviously closely packed.

Figure 2 shows the density difference between the two species along z direction in the systems with constant $N_A:N_B=1:2$, while the chain lengths are varied, i.e., N_A changes from 10 to 100. For comparison, we normalize the film thickness h to unity. It should be stressed that, here we define the film thickness of the brushes as $h=2Z_{\mathrm{cm}}$, where Z_{cm} is the distance between the center of mass of the brush chains and the grafting plane which is well defined and easily calculated.[69] In Fig. 2, we find that $\delta\rho(z)$ generally behaves similarly for different chain lengths. The curves of the long chain systems ($N_A>40$) overlap with each other very well but those with $N_A\leq40$ deviate obviously. Thus for better presenting the general behavior of polymer brush with long chain lengths, we choose the systems with $N>50$ as examples in the following simulations.

Scrutinizing Fig. 2 we can find that $\delta\rho(z)>0$ before $z/h\approx0.33$, which indicates that A chains dominate the layer from the surface to the 1/3 film height. After $z/h\approx0.33$ it is obvious that $\delta\rho(z)<0$, i.e., the B chains occupy the top 2/3 film layer. It should be noted that the maximum absolute value in the former region (slightly less than 1.0) is much smaller than that of the latter region (2.0 or so). It is easily understood that in the upper 2/3 film layer, the long B chains dominate and few A chains can stay in this layer. Intuitively we may assume $\delta\rho(z)\approx0$ in the region near to the surface, since the two components of the polymer brushes are compatible. But interestingly we can find that in such a region $\delta\rho(z)>0$, resulting in A-dominant phase. Due to the end-tethered nature of the polymer brushes, B chains have to

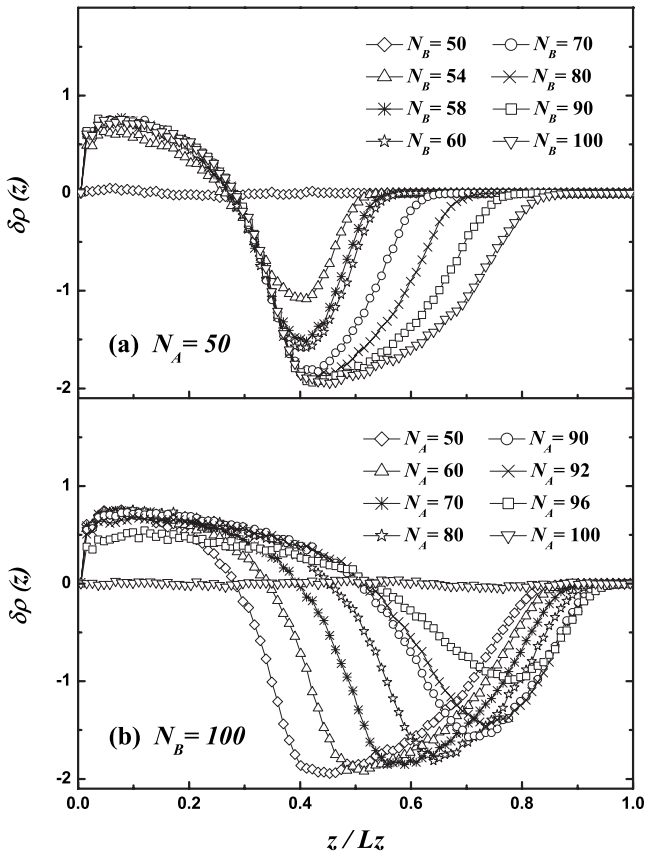

FIG. 3. The variation in the density difference profile of the two species along the z direction $\delta\rho(z)$ as a function of z/Lz in the systems with (a) N_A=50 and (b) N_B=100. Five independent samples after equilibrium are chosen to calculate the mean value and the error bar. The error bars are not shown here for clarity.

grow through the lower layer to reach the top layer. The chains are not so crowded in the top layer so the B chains possess relaxed structures and comparatively larger configurational entropy. To maximize the configuration entropy of the B chains, the A chains are compressed and parts of the B chains are stretched in the lower layer, so that $\delta\rho(z)>0$ in this region, resulting in an A-dominant phase. $z/h\approx 0.33$ sets the boundary between A-dominant phase (lower layer) and B-dominant phase (top layer), implying "phase separation" between the compatible polymer brushes.

Following the above analysis, we therefore want to know what the critical chain length difference is above which the phase separationlike layered structure can be clearly observed. Consequently we do two typical sets of simulations for our analysis: (a) N_A=50 and $N_B \in \{50,54,58,60,70,80,90,100\}$ and (b) N_B=100 and $N_A \in \{50,60,70,80,90,92,96,100\}$, respectively; the corresponding results are shown in Fig. 3(a) and 3(b), respectively. For comparing the film thickness, here we divide z coordinates by the height of the simulation box, i.e., z/Lz. As shown in Fig. 3(a), the film is much thicker in the systems with larger N_B. Comparatively, in set (b), the film thickness is only slightly increased with increasing N_A. In this set, the B chains possess longer length (N_B=100) and stay always in the top layer, thus as the A chains become longer, the lower layer of the film turns to be more and more compact. Only

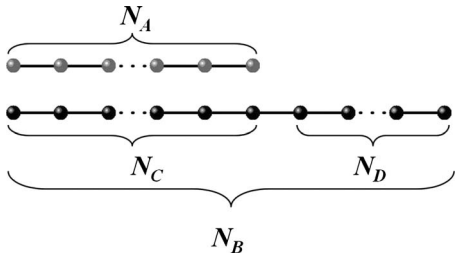

FIG. 4. A schematic illustration of different parts of B chain for the consideration of their stretch parameters in accordance with those in Fig. 5.

when the lower layer becomes compact enough can it then push the top layer higher. Therefore, we observe a much slower increase of film height with increasing chain length in set (b). Besides, in the systems of set (a), we find the positions that $\delta\rho(z)$ changing from negative to positive are equivalent ($z/Lz\approx 0.3$), which implies that the phase boundary between A-dominant and B-dominant layers in these systems are at the same height. Moreover, in the lower A-dominant layer, the absolute maximum values of $\delta\rho(z)$ are generally identical, as shown in Fig. 3(a). It is attributed to that the stretched stems of the pierced B chains through the A-dominant layer never change with the B chain length variation. On the other hand, as shown in Fig. 3(b), the changing point of $\delta\rho(z)$ raises with increasing N_A in set (b). This is because the longer the A chains are, the thicker the lower A-dominant layer should be. In these two sets we also capture that when $\Delta N\geq 20$, the absolute value of $\delta\rho(z)$ in the B layer could reach similar maximum. For example, the curves with $N_B\geq 70$ in set (a) and those with $N_A\leq 80$ in set (b) generally share the same maximum $\delta\rho(z)$ value. It reveals that the approximate critical chain length difference should be ΔN=20, above which apparent layered structures can be observed.

To characterize the conformational details of different types of chains, we define chain stretch parameter[69]

$$\phi_s = \frac{\langle R_g^z\rangle}{\left[\frac{1}{2}(\langle R_g^x\rangle + \langle R_g^y\rangle)\right]}, \tag{5}$$

where R_g^x, R_g^y, and R_g^z are the radius of gyration of the brush chain in x, y, and z directions. The value of ϕ_s indicates the degree of the chain stretching. ϕ_s=1 corresponds to a chain with spherical coil configuration and $\phi_s>1$ denotes that the chain generally stretches along the z direction. Here we consider the stretch parameter of A and B type chains, and also that of different parts of B chain, i.e., the lower part (marked as C, $N_C=N_A$) and the upper part (marked as D, $N_D=N_B-N_A$) (see Fig. 4). Figures 5(a) and 5(b) show the stretch parameters for the two sets of systems illustrated by Figs. 3(a) and 3(b), respectively. As shown in Fig. 5, $\phi_s(A)=\phi_s(B)$ for the polymer brushes with $N_A=N_B=50$ and $N_A=N_B=100$, since the two brush components are essentially identical in these two systems. It should be noted that $\phi_s=4.7$ in the case of $N_A=N_B=50$ but $\phi_s=6.7$ for $N_A=N_B=100$. In our cases, the graft density is very high (σ=1) so the chains are forced to stretch upwards. As a result, the chain configurations deviate far from Gaussian. For longer chains, R_g^z should be large but R_g^x and R_g^y are small and do not

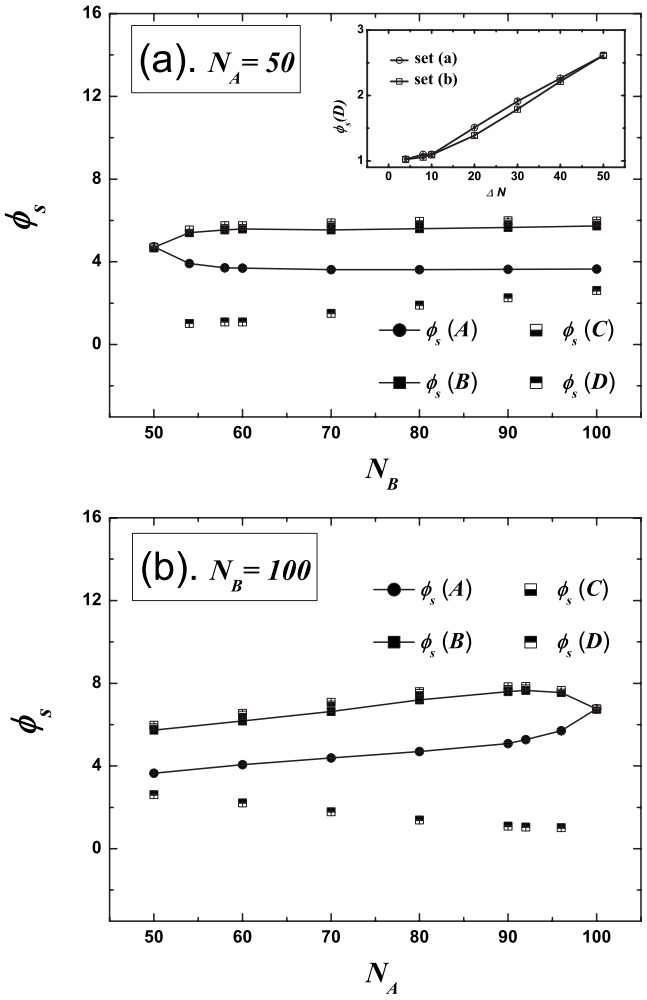

FIG. 5. The stretch parameters ϕ_s of the binary chains vs the variation in the chain lengths: (a) $N_A=50$ while N_B increases from 50 to 100 and (b) $N_B=100$ while N_A increases from 50 to 100. The solid circles stand for $\phi_s(A)$, the solid squares for $\phi_s(B)$, the lower part solid squares for $\phi_s(C)$, and the upper part solid squares for $\phi_s(D)$. Inset of (a): The variation of $\phi_s(D)$ as a function of the chain length difference ΔN. Five independent samples after equilibrium are chosen to calculate the mean values and the error bars.

change much, therefore ϕ_s for $N_A=N_B=100$ is larger than that for $N_A=N_B=50$. In set (a), $N_A=50$ while N_B increases from 50 to 100. It is shown in Fig. 5(a) that with increasing N_B, $\phi_s(A)$ decreases but $\phi_s(B)$ increases before $N_B \leq 60$. After that $\phi_s(A)$ and $\phi_s(B)$ do not change with increasing N_B. This result proves that as A chains in the lower layer can "feel" the covering of more B chains above them, A chains turn to be more compressed and B chains turn to be more stretched, so the layered structure becomes more obvious. When $\Delta N>10$, A chains in the lower compressed layer cannot feel further increase of the B chain lengths so $\phi_s(A)$ will stop decreasing. For B chains, the environment in the uncrowded top layer does not change much, thus $\phi_s(B)$ also keeps roughly constant. Moreover, $\phi_s(C)$ for the lower part of the B chains is always larger than $\phi_s(B)$. When $N_B>N_A$, to maximize the configuration entropy of the B chains, they have to grow through the lower layer dominated by the compressed A chains and allow for more B segments above the lower crowded region. Therefore, the lower parts of the B chains are much stretched. For the upper part of B chains, $\phi_s(D)$ always keeps at a much smaller value. After the B chains have grown through the A-dominant layer, they are not so crowded anymore. Therefore the upper parts of B chains tend to possess the relaxed configurations with more entropy. In the top layer, the graft density $\sigma \approx 0.5$, which is still a relatively high value [see Fig. 9(a) of Ref. 69], thus $\phi_s(D)$ stays at a value larger than 1 for $\Delta N>10$. In the region of $\Delta N<10$, the value of $\phi_s(D)$ is near 1 which is attributed to that R_g of the short chain length N_D ($N_D<10$) is comparable to the distance between itself and the around graft points, yielding a near-Gaussian property of them.

Figure 5(b) shows the stretch parameters for the systems of set (b), i.e., $N_B=100$ while N_A changes from 50 to 100. Apparently, $\phi_s(A)<\phi_s(B)$ for the system with $N_A=50$ and $N_B=100$ which are exactly corresponding to the last two points in Fig. 5(a). It can be clearly seen in Fig. 5(b) that with increasing N_A, $\phi_s(A)$ and $\phi_s(B)$ both increase linearly when $\Delta N>10$, while after $N_A>90$, $\phi_s(A)$ increases but $\phi_s(B)$ decreases until $\phi_s(A)=\phi_s(B)$ for $N_A=N_B=100$. The lower layer of the film is thickened with increasing N_A and the environment for the chains is more crowded. Hence R_g^z of the chains increases due to the crowding in the lower layer of the film. However, R_g^x and R_g^y roughly change with the variation of N_A, as a result, $\phi_s(A)$ and $\phi_s(B)$ both increase linearly when $\Delta N>10$. For $\Delta N<10$, the two kinds of chains tend to mix together thus the values of $\phi_s(A)$ and $\phi_s(B)$ get close to each other. As shown in Fig. 5, it is obvious that $\phi_s(D)$ increases with increasing ΔN. The inset of Fig. 5(a) shows the variation of $\phi_s(D)$ with increasing ΔN in the two sets of systems. We find that if ΔN is smaller than 10, the upper portions of B chains possess rather relaxed structure, showing $\phi_s(D) \approx 1$; if ΔN is larger than 10, $\phi_s(D)$ increases linearly with ΔN, showing the crowding effect.

We also note that the layered structures formed in this system are very sensitive to the chain length difference. As shown in Fig. 3, the $\delta\rho(z)$ curves for $\Delta N=0$ ($N_A=N_B=50$ and $N_A=N_B=100$) are flat, indicating a uniform film. However, a slight difference on chain lengths will induce layered structure with compressed A chains and stretched B chains. This implies a possibility that designing a film which can sensitively tune the wettability and adhesion of the surface as a response of slight environment change such as the solvent selectivity. Therefore we take the system with $N_A=50$ and $N_B=54$ as an example to study the influence of solvent selectivity on the film property. Figure 6 shows the variation of $\delta\rho(z)$ as a function of z/Lz with $N_A=50$ and $N_B=54$ in the following two sets: (c) the solvent is hydrophilic for A ($\alpha_{AS}<25$) but neutral for B ($\alpha_{BS}=25$); and (d) the solvent is hydrophobic for B ($\alpha_{BS}>25$) but neutral for A ($\alpha_{AS}=25$). In both sets, we also take the original athermal system ($\alpha_{AB}=\alpha_{AS}=\alpha_{BS}=25$, the hollow circles) as a comparison. When the solvent becomes favoring A [Fig. 6(a)] or unfavoring B [Fig. 6(b)], it is clear that the A chains tend to rise up to the top layer of the brush and the B chains collapse to the lower layer. Such a drastic switch is only based on a weak change of the solvent selectivity that $\Delta\alpha=\alpha_{BS}-\alpha_{AS}>0$ without the incompatibility between the two species. We also find that the curves corresponding to the weak solvent selectivity (the hollow squares in both sets) are flat, indicating the mixing

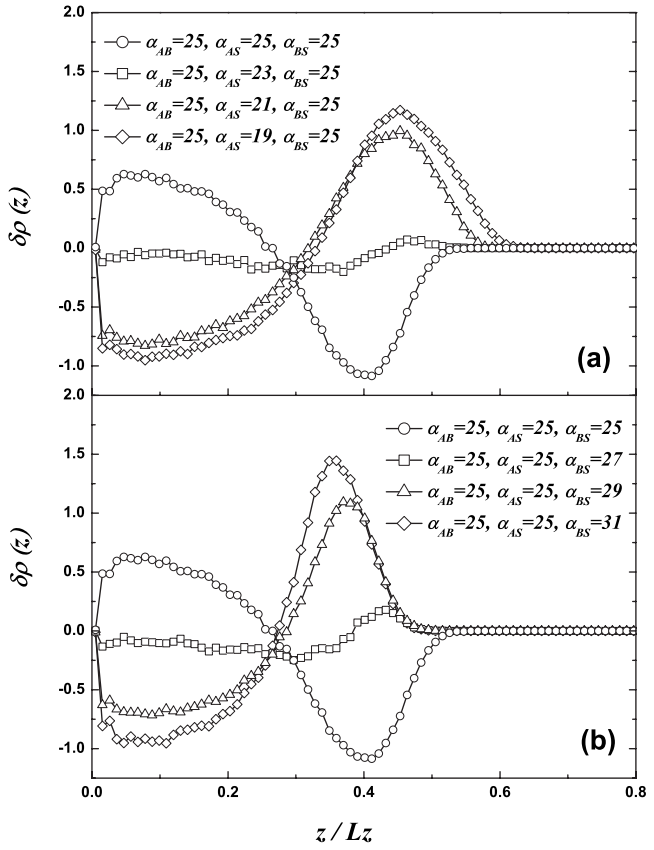

FIG. 6. The variation in the density difference profile of the two species along the z direction $\delta\rho(z)$ as a function of z/Lz in the systems with $N_A=50$ and $N_B=54$, where (a) the solvent is favoring A ($\alpha_{AS}<25$) but neutral for B ($\alpha_{BS}=25$) and (b) the solvent is "hating" B ($\alpha_{BS}>25$) but neutral for A ($\alpha_{AS}=25$). Five independent samples after equilibrium are chosen to calculate the mean values and the error bars. The error bars are not shown for clarity.

between the two components. It implies that the layered structures observed in differing chain length systems are due to phase separation, since we need extra energy to break the layered structures and mix up the brush components now. Moreover, we find in Fig. 6(a) that the film is thicker with the increase of $\Delta\alpha$. In this set, the top A-dominant layer should become much loose since the A chains are preferred by the solvent so that they could extend upwards with the preference of the solvent. Hence the system with $\alpha_{AS}=19$ is the thickest but the loosest film since $\Delta\alpha=6$ is large enough to provide sufficient driving force for the A chains stretching upwards. In Fig. 6(b), we also find that the phase switch in the systems with larger $\Delta\alpha$ are more obvious, however, the film thicknesses of the systems are almost equal. It is an unexpected result but seems plausible. The brush chains are immersed in the solvent thus the unfavored B chains would be repelled by the solvent. As a result, the lower B-dominant layer after the phase switch would turn to be more condensed, i.e., the systems in Fig. 6(b) should possess the lower B-dominant layers with the equal height. This can also be verified by the overlapping point $z/Lz\approx0.28$ where $\delta\rho(z)$ changing from negative to positive [see Fig. 6(b)]. On the other hand, the top A chains with $N_A=50$ are neutral to the solvent in these systems. Therefore, the heights of the top A layers should also be equal, thus the film thicknesses of the systems are identical. It is a significantly suggestive result that the slight change of the solvent selectivity in the system with critical ΔN could greatly switch the morphology that the short chains raise to the top but the longer chains collapse to the bottom of the film. This result implies the possibility of preparing the sensitive binary brush film in experiments that could be applied to reversibly tune the surface wettability.

IV. CONCLUSIONS

The layered structures of compatible binary brushes with high graft density are investigated using DPD simulations. The layered structures are characterized by apparent A and B dominant regions parallel to the surface, indicating a "phase separationlike" behavior. The chain conformational entropy should be the driving force of the layered structures which are found to be very sensitive to the change in the chain length difference ΔN. The stretch parameters of the binary brushes reflect diverse conformational details of different chains and even of different parts of the same chain. Moreover, we find that slight change of the solvent selectivity favoring the short chains will greatly switch the film morphology, i.e., the short chains will raise to the top but the longer chains will collapse to the bottom of the film. This result implies the possibility of preparing the sensitive binary brush film in experiments that could be applied to reversibly tune the surface wettability.

ACKNOWLEDGMENTS

This work is supported by the National Science Foundation of China (Grant Nos. 20774036, 20974040, and 50930001) and Fok Ying Tung Education Foundation (114018).

[1] S. Pal and C. Seidel, Macromol. Theory Simul. **15**, 668 (2006).
[2] C. M. Chen and Y. A. Fwu, Phys. Rev. E **63**, 011506 (2000).
[3] F. Goujon, P. Malfreyt, and D. J. Tildesley, ChemPhysChem **5**, 457 (2004).
[4] P. Malfreyt and D. J. Tildesely, Langmuir **16**, 4732 (2000).
[5] C. Pastorino, K. Binder, T. Kreer, and M. Müller, J. Chem. Phys. **124**, 064902 (2006).
[6] S. Alexander, J. Phys. (Paris) **38**, 983 (1977).
[7] P. G. de Gennes, Macromolecules **13**, 1069 (1980).
[8] P. G. de Gennes, Adv. Colloid Interface Sci. **27**, 189 (1987).
[9] S. T. Milner, T. A. Witten, and M. E. Cates, Macromolecules **21**, 2610 (1988).
[10] S. T. Milner, Science **251**, 905 (1991).
[11] D. V. Kuznetsov and Z. Y. Chen, J. Chem. Phys. **109**, 7017 (1998).
[12] D. Irfachsyad, D. Tildesley, and P. Malfreyt, Phys. Chem. Chem. Phys. **4**, 3008 (2002).
[13] C. M. Wijmans and B. Smit, Macromolecules **35**, 7138 (2002).
[14] M. Murat and G. S. Grest, Phys. Rev. Lett. **63**, 1074 (1989).
[15] R. Dickman and P. E. Anderson, J. Chem. Phys. **99**, 3112 (1993).
[16] P. Y. Lai and E. B. Zhulina, Macromolecules **25**, 5201 (1992).
[17] P. Y. Lai and K. Binder, J. Chem. Phys. **98**, 2366 (1993).
[18] P. Y. Lai and K. Binder, J. Chem. Phys. **95**, 9288 (1991).
[19] P. Y. Lai and K. Binder, J. Chem. Phys. **97**, 586 (1992).
[20] G. S. Grest, J. Chem. Phys. **105**, 5532 (1996).
[21] P. S. Doyle, E. S. G. Shaqfeh, and A. P. Gast, Macromolecules **31**, 5474 (1998).
[22] K. C. Daoulas, A. F. Terzis, and V. G. Mavrantzas, J. Chem. Phys. **116**, 11028 (2002).
[23] M. Laradji, H. Guo, and M. J. Zuckermann, Phys. Rev. E **49**, 3199 (1994).

[24] A. Karim, S. K. Satija, J. F. Douglas, J. F. Ankner, and L. J. Fetters, Phys. Rev. Lett. **73**, 3407 (1994).
[25] T. J. Hu and C. Wu, Phys. Rev. Lett. **83**, 4105 (1999).
[26] G. Hadziioannou, S. Patel, S. Granick, and M. Tirrell, J. Am. Chem. Soc. **108**, 2869 (1986).
[27] H. J. Taunton, C. Toprakcioglu, L. J. Fetters, and J. Klein, Nature (London) **332**, 712 (1988).
[28] H. J. Taunton, C. Toprakcioglu, L. J. Fetters, and J. Klein, Macromolecules **23**, 571 (1990).
[29] T. Cosgrove, J. Chem. Soc., Faraday Trans. **86**, 1323 (1990).
[30] P. Auroy, L. Auvray, and L. Léger, Phys. Rev. Lett. **66**, 719 (1991).
[31] S. Patel and M. Tirrell, Annu. Rev. Phys. Chem. **40**, 597 (1989).
[32] S. Yamamoto, M. Ejaz, Y. Tsujii, and T. Fukuda, Macromolecules **33**, 5608 (2000).
[33] S. Yamamoto, Y. Tsujii, and T. Fukuda, Macromolecules **33**, 5995 (2000).
[34] H. W. Ma, J. H. Hyun, P. Stiller, and A. Chilkoti, Adv. Mater. **16**, 338 (2004).
[35] D. M. Jones, A. A. Brown, and W. T. S. Huck, Langmuir **18**, 1265 (2002).
[36] L. Wenning, M. Müller, and K. Binder, Europhys. Lett. **71**, 639 (2005).
[37] M. Motornov, R. Sheparovych, R. Lupitskyy, E. MacWilliams, and S. Minko, J. Colloid Interface Sci. **310**, 481 (2007).
[38] P. Uhlmann, L. Ionov, N. Houbenov, M. Nitschke, K. Grundke, M. Motornov, S. Minko, and M. Stamm, Prog. Org. Coat. **55**, 168 (2006).
[39] P. Uhlmann, N. Houbenov, N. Brenner, K. Grundke, S. Burkert, and M. Stamm, Langmuir **23**, 57 (2007).
[40] A. Sidorenko, S. Minko, K. Schenk-Meuser, H. Duschner, and M. Stamm, Langmuir **15**, 8349 (1999).
[41] S. Minko, M. Müller, D. Usov, A. Scholl, C. Froeck, and M. Stamm, Phys. Rev. Lett. **88**, 035502 (2002).
[42] S. Minko, M. Müller, M. Motoronov, M. Nitschke, K. Grundke, and M. Stamm, J. Am. Chem. Soc. **125**, 3896 (2003).
[43] L. Ionov, S. Minko, M. Stamm, J. F. Gohy, R. Jerome, and A. Scholl, J. Am. Chem. Soc. **125**, 8302 (2003).
[44] J. F. Marko and T. A. Witten, Phys. Rev. Lett. **66**, 1541 (1991).
[45] J. F. Marko and T. A. Witten, Macromolecules **25**, 296 (1992).
[46] M. Müller, Phys. Rev. E **65**, 030802(R) (2002).
[47] M. W. Matsen and M. Schick, Phys. Rev. Lett. **72**, 2660 (1994).
[48] C. Singh, G. T. Pickett, E. Zhulina, and A. C. Balazs, J. Phys. Chem. B **101**, 10614 (1997).
[49] H. Dong, J. Phys. II **3**, 999 (1993).
[50] E. Zhulina and A. C. Balazs, Macromolecules **29**, 2667 (1996).
[51] G. Brown, A. Chakrabarti, and J. F. Marko, Europhys. Lett. **25**, 239 (1994).
[52] P. Y. Lai, J. Chem. Phys. **100**, 3351 (1994).
[53] K. G. Soga, M. J. Zuckermann, and H. Guo, Macromolecules **29**, 1998 (1996).
[54] H. Merlitz, G. L. He, J. U. Sommer, and C. X. Wu, Macromolecules **42**, 445 (2009).
[55] G. L. He, H. Merlitz, J. U. Sommer, and C. X. Wu, Macromolecules **42**, 7194 (2009).
[56] B. Zhao, R. T. Haasch, and S. MacLaren, J. Am. Chem. Soc. **126**, 6124 (2004).
[57] S. Minko, S. Patil, V. Datsyuk, F. Simon, K. J. Eichhorn, M. Motornov, D. Usov, I. Tokarev, and M. Stamm, Langmuir **18**, 289 (2002).
[58] M. Lemieux, S. Minko, D. Usov, M. Stamm, and V. V. Tsukruk, Langmuir **19**, 6126 (2003).
[59] R. Magerle, Phys. Rev. Lett. **85**, 2749 (2000).
[60] D. Usov, V. Gruzdev, M. Nitschke, M. Stamm, O. Hoy, I. Luzinov, I. Tokarev, and S. Minko, Macromolecules **40**, 8774 (2007).
[61] S. Santer, A. Kopyshev, H. K. Yang, and J. Rühe, Macromolecules **39**, 3056 (2006).
[62] R. Sheparovych, M. Motornov, and S. Minko, Langmuir **24**, 13828 (2008).
[63] A. M. Skvortsov, L. I. Klushin, and A. A. Gorbunov, Macromolecules **30**, 1818 (1997).
[64] H. Merlitz, G. L. He, C. X. Wu, and J. U. Sommer, Macromolecules **41**, 5070 (2008).
[65] H. Merlitz, G. L. He, C. X. Wu, and J. U. Sommer, Phys. Rev. Lett. **102**, 115702 (2009).
[66] R. D. Groot and P. B. Warren, J. Chem. Phys. **107**, 4423 (1997).
[67] P. Español and P. B. Warren, Europhys. Lett. **30**, 191 (1995).
[68] R. D. Groot and T. J. Madden, J. Chem. Phys. **108**, 8713 (1998).
[69] H. Liu, M. Li, Z. Y. Lu, Z. G. Zhang, and C. C. Sun, Macromolecules **42**, 2863 (2009).
[70] I. V. Pivkin and G. E. Karniadakis, J. Comput. Phys. **207**, 114 (2005).